ELSEVIER

European Journal of Pharmacology 363 (1998) 81–90

ejp

Inhibition by local anesthetics of Ca^{2+} channels in rat anterior pituitary cells

Zhiling Xiong [a,b], Gary R. Strichartz [a,b,*]

[a] *Pain Research Center, Department of Anesthesia, Brigham and Women's Hospital, Harvard Medical School, 75 Francis Street, Boston, MA 02115 USA*
[b] *Department of Biological Chemistry and Molecular Pharmacology, Harvard Medical School, Boston, MA 02115 USA*

Received 9 October 1998; accepted 20 October 1998

Abstract

The characteristics of local anesthetic inhibition of voltage-dependent Ca^{2+} channels in a rat pituitary clonal cell line were investigated by whole-cell voltage clamp and compared with inhibition by the dihydropyridine Ca^{2+} channel antagonist, nicardipine. With extracellular Ba^{2+} (10 mM) as the current carrier, depolarization above −40 mV evoked a slowly inactivating I_{Ba}. Extracellularly applied lidocaine inhibited I_{Ba} without changing the activation threshold, the voltage of peak current, or the reversal potential. Inhibition was greater at a holding potential of −60 mV ($IC_{50} = 1.2$ mM) than at −80 mV ($IC_{50} = 2.6$ mM). This depolarization-induced potentiation in I_{Ba} inhibition developed over 0.1–10 s after membrane depolarization began. Nicardipine also dose-dependently inhibited I_{Ba} with an $IC_{50} = 90$ nM (at a holding potential = −80 mV). Both lidocaine and nicardipine shifted the I_{Ba} steady-state inactivation (availability) curves to the left. Double-pulse protocols revealed that lidocaine (1 mM) accelerated the depolarization-induced inhibition (inactivation) of I_{Ba} over the rate in drug-free solutions, but had no effect on the hyperpolarization-induced removal of channel inactivation. Nicardipine also accelerated the depolarization-induced inactivation of I_{Ba} but, in addition, it slowed the hyperpolarization-induced inactivation removal. The relative inhibitory action of lidocaine in suppressing I_{Ba} was unchanged in the presence of nicardipine. These results suggest that lidocaine has a direct action on membrane Ca^{2+} channels, similar to the voltage-dependent action of dihydropyridine, but acting at a separate and independent site.

Keywords: Ca^{2+} channel; Lidocaine; Bupivacaine; Nicardipine; Voltage clamp, whole-cell; GH_3 cell

1. Introduction

Local anesthetics, in their therapeutic actions as impulse blockers and anti-arrhythmics, act on the voltage-gated sodium channels of nerve and cardiac muscle, respectively (Taylor, 1959; Weidmann, 1955). Local anesthetic molecules bind to the different conformational 'states' of channels with different affinities (Hille, 1977) to either prevent or reduce neuronal impulse propagation, or to limit the frequency of myocardial action potentials and so prevent tachyrhythmias (Hondeghem and Katzung, 1977). Because of the state-dependence of the functional affinities that underlie these different actions, the effective concentrations differ markedly between tissues. For example, complete neuronal impulse inhibition requires ca. 10^{-3} M lidocaine at the nerve (Fink and Cairns, 1987; Huang et al., 1997) whereas the antiarrhythmic actions occur at ca. 10^{-5} M (Kessler et al., 1984) intravenous lidocaine.

Proteins other than Na^+ channels also can be affected by local anesthetics. A variety of transport enzymes, phospholipases, and even the microtubules supporting axonal transport, as well as K^+ and Ca^{2+} channels in excitable and secretory cells are altered by these drugs (for review, see Butterworth and Strichartz, 1990). Several of these other proteins may be affected by local anesthetics in therapeutic applications where the actions on Na^+ channels alone provide an inadequate or incomplete explanation. Specific examples occur in spinal or epidural anesthesia, where the entire spinal cord is surrounded by cerebrospinal fluid containing high concentrations of drug (Cohen, 1968), and in the intravenous use of local anesthetics for relief of chronic pain wherein very low concentrations of drug are effective (Chaplan et al., 1995). Furthermore, in most applications of local anesthetics, vascular physiology is often modified, either through the effects on innervating autonomic nerves (Kalman et al., 1997) or

* Corresponding author. Tel.: +1-617-732-8797; Fax: +1-617-730-2801; E-mail: gstrichz@zeus.bwh.harvard.edu

0014-2999/98/$ - see front matter
PII: S0014-2999(98)00769-9

directly on the vascular endothelial and smooth muscle cells (Johns et al., 1985; Partridge, 1991).

In this study we investigated the actions of the lidocaine and bupivacaine on the voltage-dependent Ca^{2+} channels. The actions of local anesthetics on Ca^{2+} currents in skeletal (Palade and Almers, 1985) and cardiac (Josephson, 1988; Carmeliet et al., 1986; Wulf et al., 1994; Rossner and Freese, 1997) muscle and in sensory neurons (Bingmann et al., 1987; Guo et al., 1991; Sugiyama and Muteki, 1994) have been reported previously. Here we chose to examine these actions on the L-type Ca^{2+} channels in rat anterior pituitary (GH_3 clonal) cells. We sought to investigate any use-dependent actions, to characterize rates of drug binding and dissociation, and to compare the inhibition by local anesthetics with those of dihydropyridines, classic selective inhibitors of L-type Ca^{2+} channels. We also sought electrophysiological data for any functional competition between local anesthetics and dihydropyridines, since several publications have reported that dihydropyridine binding is inhibited by local anesthetics (Bolger et al., 1987; Browne et al., 1996). A brief report of these results was presented at a Biophysical Society meeting (Xiong and Strichartz, 1995).

2. Materials and methods

2.1. Cell culture

Clonal rat pituitary (GH_3) cells were purchased from the American Type Culture Collection and cultured as described previously (Dubinsky and Oxford, 1985). Briefly, cells were grown on 12 mm glass coverslips placed in 35 mm plastic tissue culture dishes. Media used is 89% Dulbecco's Eagle Medium (Gibco cat. # 11965), supplemented with 1% penicillin-streptomycin (Gibco cat. 15140) and 10% fetal bovine serum (HyClone cat. # A-1111). Cells were kept in a humidified incubator at 37°C in 5% CO_2/95% air mixture. They were replated to a lower density every seven days, and the culture medium was changed on the third or fourth day after replating.

2.2. Electrophysiology

The methods used to record the whole-cell membrane currents were similar to those described previously (Hamill et al., 1981; Cohen and McCarthy, 1987). The coverslip with cells attached was placed in a small chamber (0.6 ml) positioned on the stage of a differential interference inverted microscope (IMT-2, Olympus, Tokyo, Japan). Only round cells with total cell capacitance of 15–40 pF (mostly 20–30 pF, determined by integration of capacitive current required for step hyperpolarization, and ca. 15–25 μm in diameter) were used. The chamber was then perfused continuously during experimentation at a flow rate of 2 ml/min. Drugs were flushed onto the voltage-clamped cell through 0.2 mm (i.d.) glass tubes placed 0.2 mm away from the cell; the microperfusion flow rate was 100 μl/min. All experiments were performed at room temperature (22–24°C).

Whole-cell voltage clamp was performed with patch electrodes with resistances of 0.8–2 MΩ made from borosilicate glass capillary tubing (World Precision Instruments, Sarasota, FL) using a patch-clamp amplifier (Axopatch-200, Axon Instruments, Foster City, CA). After making a giga-seal (> 10 GΩ), the patch membrane was ruptured by negative pressure (10–20 mm H_2O). Series resistance (R_s, 1.5–5 MΩ) was partly (70–80%) compensated electrically. The current signal from the amplifier was filtered at 2 kHz (4-pole Bessel filter). Leak and residual capacitive currents were subtracted using the 'P/4' procedure (Bezanilla and Armstrong, 1977). The data were recorded and analyzed using pClamp software (Axon Instruments). Averaged values are reported as means ± S.E.M.

2.3. Solutions

To eliminate K^+ currents, the pipette was filled with a high $[Cs^+]$ solution of the following composition (in mM): 110 CsCl, 20 tetraethylammonium chloride (TEA-Cl), 5 $MgCl_2$, 5 Na_2ATP, 4 ethyleneglycol-bis(B-aminoethylether)-*N*,*N*,*N*′,*N*′-tetraacetic acid (EGTA), 10 *N*-(2-hydroxyethl)piperazine-*N*-2-ethanesulphonic acid (HEPES). The nominally Ca^{2+}-free external solution for 'sealing' contained (in mM): 137 TEACl, 6 KCl, 1.2 $MgCl_2$, 10 glucose, 10 HEPES. The 10 mM Ba^{2+} solution used for recording Ba^{2+} current contained (in mM): 130 TEACl, 10 $BaCl_2$, 10 glucose, 10 HEPES. Tetrodotoxin (1 μM) was also added in the solution to eliminate Na^+ channel current (I_{Na}). In a few experiments, 10 mM Ca^{2+} solution was used; in these cases, Ba^{2+} was replaced by equimolar Ca^{2+}. To record I_{Na}, a high Na^+ bath solution was used with the following composition (in mM): 140 NaCl, 6 KCl, 2 $MnCl_2$, 10 Glucose, 10 HEPES. The pH was adjusted to 7.2 for the pipette solution, and 7.30–7.35 for all bath solutions with tris(hydroxymethyl)aminomethane (Tris).

2.4. Drugs

The drugs used were lidocaine · HCl, bupivacaine · HCl, nicardipine (Sigma, St. Louis, MO), and tetrodotoxin (Calbiochem, San Diego, CA), and ω-conotoxin (Alomone Labs, Jerusalem, Israel). Lidocaine, tetrodotoxin, and ω-conotoxin were dissolved in distilled water. Bupivacaine was dissolved in dimethylsulfoxide (DMSO), and nicardipine was dissolved in 50% ethanol, the container wrapped in aluminum foil, and stored at 4°C. The final maximal concentration of either DMSO or ethanol was demonstrated to have no affect on the Ca^{2+} channel currents (data not shown).

3. Results

3.1. Ca^{2+} channel currents in anterior pituitary cells

The slow inward current in GH_3 cells, activating at potentials > -50 mV, exhibited little inactivation over the duration of the depolarizing pulse (300 ms) when the charge carrier was Ba^{2+} (see Figs. 1A and 2). Removal of Ca^{2+} or Ba^{2+} ion from the bathing solution caused this current to disappear, and both extracellular Mn^{2+} (2 mM) and nicardipine (1–10 μM) totally abolished the inward current. The addition of ω-conotoxin (1 μM) had no detectable effect on I_{Ba} in these cells. These results indicate that the inward current was carried by Ca^{2+} or Ba^{2+}, almost exclusively through L-type Ca^{2+} channels.

In the present study, Ba^{2+} was used as the major charge carrier since: (1) Ba^{2+} produced 2 times larger inward Ca^{2+} channel currents than Ca^{2+} did and (2) Ba^{2+} slowed the speed of Ca^{2+} channel rundown. In control experiments, Ba^{2+} current (I_{Ba}) in most of the cells exhibited a small (less than 10%) rundown for 20 min at a HP of -80 mV. In addition, in some cells the relatively 'stable' I_{Ba}

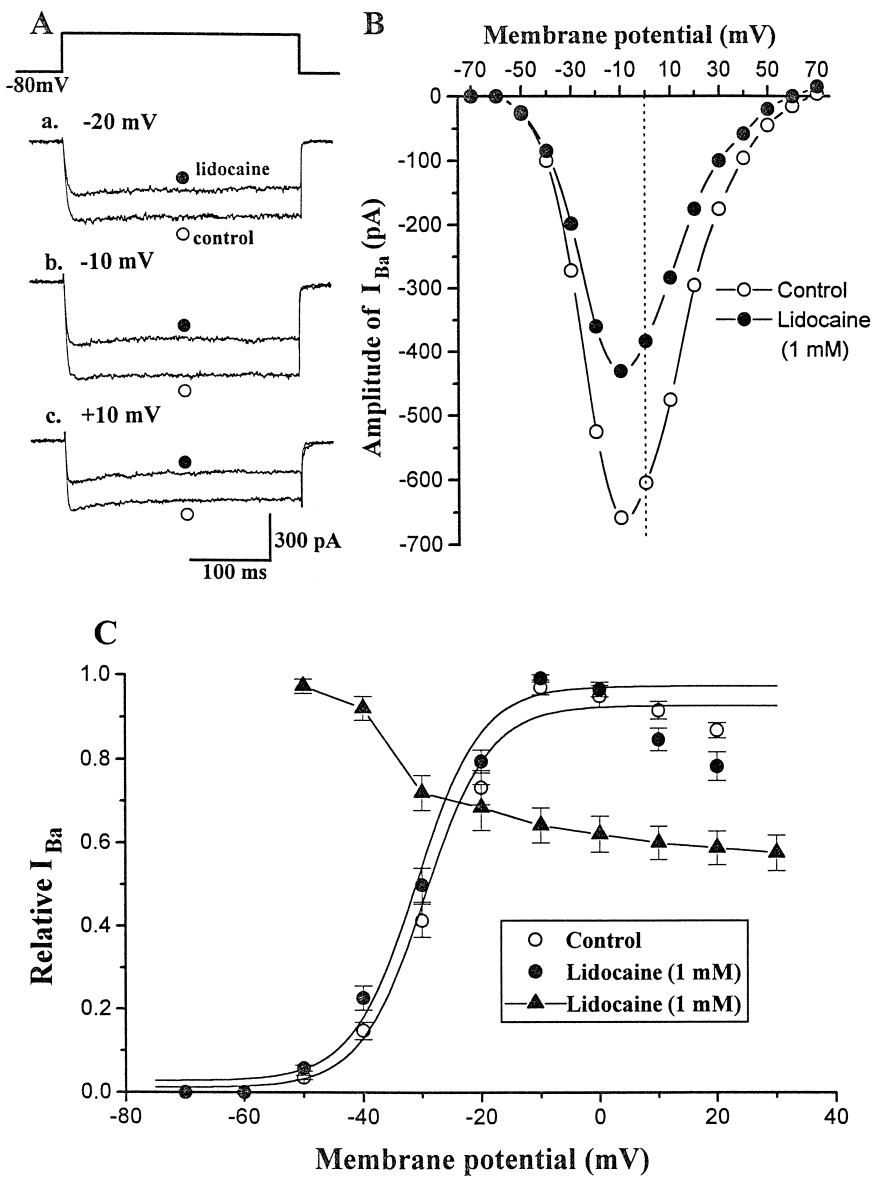

Fig. 1. Inhibitory effect of lidocaine on Ca^{2+} channels. The intracellular pipette was filled with high Cs^+ solution, and the bath was superfused with 10 mM Ba^{2+} solution. Holding potential $= -80$ mV. (A) Representative Ba^{2+} currents in the absence (open circles) and presence (filled circles) of 1 mM lidocaine. (B) Ba^{2+} current–voltage relationship of in the absence (open circles) and presence (filled circles) of 1 mM lidocaine. (A) and (B) were from the same cell. (C) Peak activation curves in the absence (open circles) and presence (filled circles) of 1 mM lidocaine ($n = 5$). The activation curves are fitted by the Boltzmann equation of the form: $I = 1/\{1 + \exp[(V - V_{0.5})/k]\}$, where $V_{0.5}$ is the voltage for half-activation, and k is the slope of the curve. For control: $V_{0.5} = -29.7$ mV, and $k = 5.4$ mV; for lidocaine: $V_{0.5} = -31.1$ mV, and $k = 5.4$ mV. Inhibition of peak I_{Ba} by lidocaine (1 mM) at various test potentials, (filled triangles, $n = 6$) was calculated as the ratio of current in lidocaine to control current.

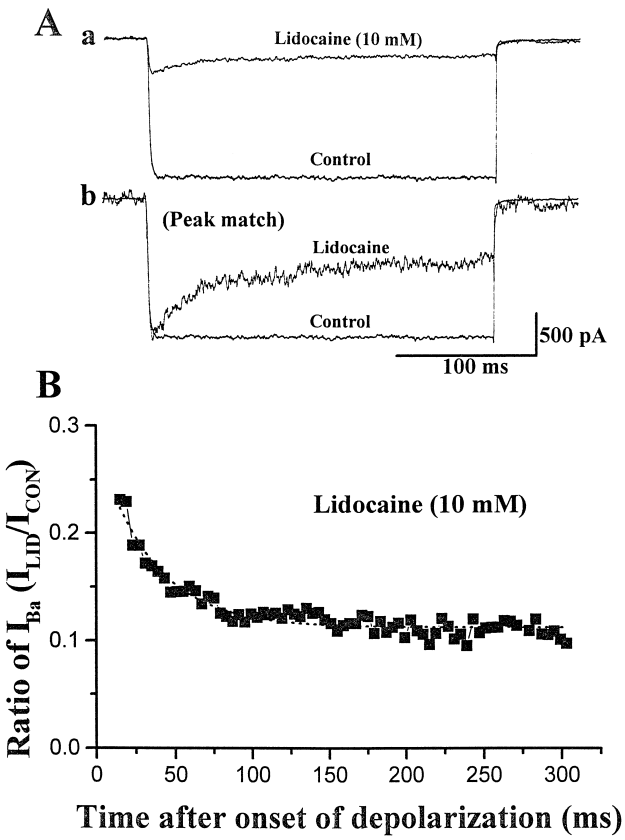

Fig. 2. Time-dependent inhibition of I_{Ba} by lidocaine. Experimental conditions were the same as in Fig. 1. (A) Superimposed I_{Ba} traces in the absence and presence of 10 mM lidocaine before (a) and after (b) the scaling for peak current match. (B) Ratio of I_{Ba} (lidocaine): I_{Ba} (control) during the test depolarization to −10 mV. Points are data from Fig. 2A; dotted line is a nonlinear least-squares fit of a single exponential to the data.

could be recorded for 40 min with minimal (5–10%) rundown. Those cells which showed quick rundown (usually apparent within 10 min) were discarded.

3.2. Inhibitory effect of lidocaine on I_{Ba}

Upon extracellular application of lidocaine (1 mM), I_{Ba} was significantly inhibited (Fig. 1A). The full current–voltage relationship of this inhibition is shown in Fig. 1B. Lidocaine depressed peak I_{Ba} over the voltage range of −40 to +60 mV without changing the activation threshold, the voltage of peak current, or the reversal potential. Inhibition increased steeply with voltage in the range of channel activation, −50 to −20 mV, and then more gradually as the test potential became more positive (Fig. 1C). The small currents clearly detectable at −50 mV were unaffected by 1 mM lidocaine.

Voltage-dependent activation (g_{Ba}) was determined from the peak I_{Ba}, using the Ohmic approximation: $g_{Ba} = I_{Ba}/(E_{Rev} - E_m)$, where E_{Rev} is the reversal potential, and E_m is the test potential at which I_{Ba} is evoked. As shown in Fig. 1C, voltage-dependence of activation of I_{Ba} (normalized to 1.0 by the maximum current at 10 mV) is little affected by lidocaine at 1 mM.

In addition, inhibition of I_{Ba} by lidocaine increased slightly during the 300 ms long test depolarization, a phenomenon especially apparent at higher drug concentrations (3.3 and 10 mM). As shown in Fig. 2, I_{Ba} decayed little in the absence of drug. After application of lidocaine (10 mM), I_{Ba} was strongly inhibited at the start of the test potential and even more so at the end (Fig. 2Aa). This phenomenon is more obvious when the peak I_{Ba} of both traces are matched by scaling the lidocaine-depressed current to the control peak amplitude (Fig. 2Ab). (Similar results were also obtained with nicardipine (data not shown)).

The kinetics of the ratio of I_{Ba} with lidocaine to I_{Ba} control during the pulse (from 15 to 300 ms) could be fit well by a single exponential (with $\tau = 35$ ms, Fig. 2B). (In these experiments, the current ratio for the first 15 ms of the pulse was not measured because the electrical capacity and the $P/4$ subtraction might contaminate the initial time course of the I_{Ba} decay.) The fractional blockade for the peak of the current was 0.76 and represents the degree of inhibition by 10 mM lidocaine of resting, closed Ca^{2+} channels. The corresponding K_d for lidocaine's blocking/binding is ca. 3.1 mM, assuming that 1 lidocaine molecule blocks 1 channel. The further blockade of Ca^{2+} channels that occurs during depolarization-induced channel opening strengthens the inhibition to 90%, which corresponds to a K_d of 1.1 mM. The kinetic scheme of the drug (L) and open (O) or resting (R) Ca^{2+} channels used to model this phenomenon is:

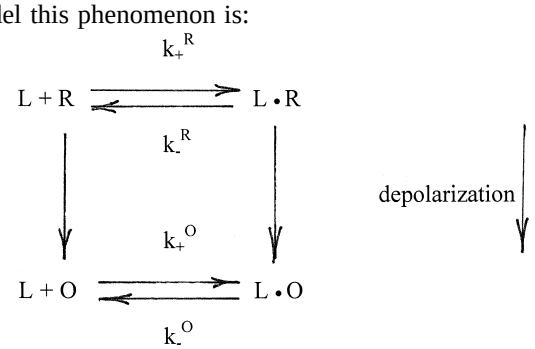

(1)

Assuming that the additional binding that occurs following depolarization involves only open channels, i.e., that $L \cdot R$ goes to $L \cdot O$ as rapidly as R goes to O, then the combination of the time constant (35 ms) and the K_d (1.1 mM) can be used to calculate the forward and reverse rate constants for open channel block, k_+^O, k_-^O, respectively, through the equations:

$$\tau^{-1} = \left(k_+^O[L] + k_-^O\right) \quad (2)$$

$$K_d = k_-^O/k_+^O \quad (3)$$

Accordingly, $k_+^O = 2.57 \times 10^3\ M^{-1}\ s^{-1}$, and $k_-^O = 2.83\ s^{-1}$. Similar rate constant values were derived from the

depolarization-induced (open channel) block in 3.3 mM lidocaine.

3.3. Influence of holding potential on lidocaine's potency

The inhibition by lidocaine of Ca^{2+} channel current decreased at more negative holding potentials. Lidocaine (3 mM) inhibited peak I_{Ba} more at the holding potential of −60 mV (57%) than at −80 mV (38%). Steady-state I_{Ba} at the end of a 300 ms test depolarization was inhibited by 75% and 57% at −60 mV and −80 mV holding potentials, respectively, about the same ratio of inhibition as for the 'peak' I_{Ba} (data not shown). In addition, after washing out lidocaine for 5 min at the holding potential of −80 mV, I_{Ba} recovered almost completely to the control levels, whereas at −60 mV recovery was slower and less complete after 5 min.

A full lidocaine concentration–inhibition curve at two different holding potentials is shown in Fig. 3. The potency for inhibition was greater at −60 mV ($IC_{50} = 1.2$ mM for peak current) than at −80 mV ($IC_{50} = 2.6$ mM). The concentration–response relationships for both potentials are fit well by a Hill equation with a coefficient, n, of about 1 (see figure legend), consistent with lidocaine having a single inhibitory binding site on Ca^{2+} channels.

3.4. Steady-state inactivation of I_{Ba}

To further characterize the voltage dependence of the Ca^{2+} channel inhibition, the steady-state inactivation of I_{Ba} was examined in the absence and presence of lidocaine or nicardipine. Steady-state inactivation of I_{Ba} was determined using a two-pulse protocol in which the potential was set to various 'conditioning' levels from −100 to +20 mV and then, after a short interval (20 ms) at −80 mV, shifted to a test potential of −10 mV (see Fig. 4 inset). The absolute (Fig. 4A) and the relative (Fig. 4B) amplitude of peak I_{Ba} was plotted against the conditioning potentials, and the curve was fitted to the data by a Boltzmann equation of the form:

$$I = 1/\{1 + \exp[(V - V_{0.5})/k]\} \quad (4)$$

where $V_{0.5}$ is the voltage for half-inactivation, and k is the Boltzmann coefficient (slope of the curve).

At first we used a 5 s conditioning pulse to assess the availability (1-inactivation) of I_{Ba} in the absence and presence of lidocaine (or nicardipine). Lidocaine (1 mM) shifted this availability curve to the left by about 7 mV ($V_{0.5} = -33.6 \pm 3.1$ mV for control, and -40.2 ± 3.6 mV for lidocaine, $n = 5$, $P < 0.05$). Nicardipine (100 nM) also shifted the availability curve to the left, by 15 mV ($V_{0.5}$ was -32.9 ± 2.8 mV for control, and -47.9 ± 3.2 mV

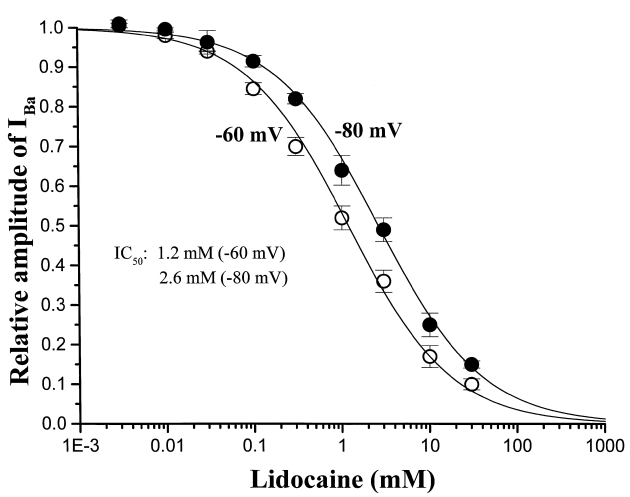

Fig. 3. Concentration dependence of lidocaine inhibition of peak I_{Ba} at two different holding potentials. Currents evoked at −10 mV from either −80 or −60 mV. Each symbol and vertical bar represents means ± S.E., respectively. Data at each point were from 6–12 cells. The solid lines are nonlinear least-squares fits of the Hill equation:

$$\text{Relative } I_{Ba} = 1 - [\text{lidocaine}]^n / \{[\text{lidocaine}]^n + K_d^n\}.$$

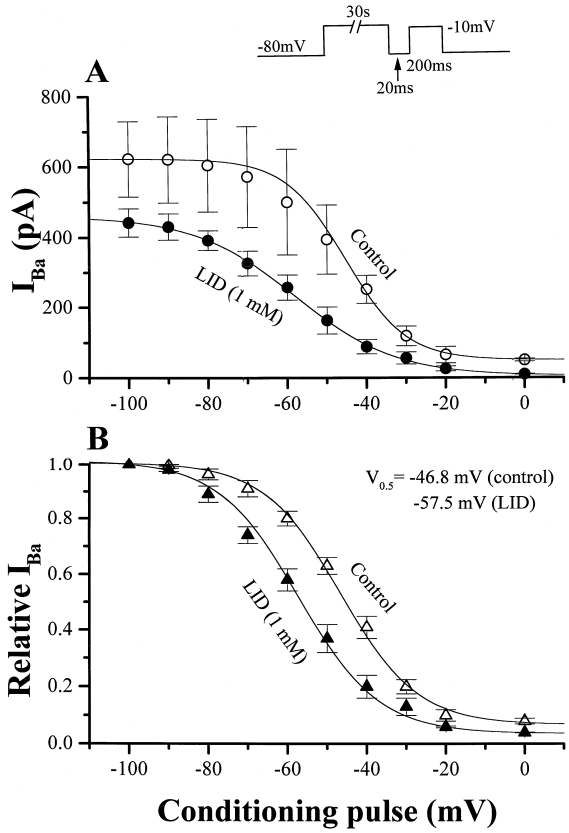

Fig. 4. Steady-state inactivation of I_{Ba} in the absence (open symbols) and presence (filled symbols) of 1 mM lidocaine. Experimental protocol is shown in the upper right corner. (A) Absolute changes of I_{Ba}. (B) Relative changes of I_{Ba}. The solid curves are fits of Eq. (2) (see text) to the data: $V_{0.5}$ and k, respectively, equaled -46.8 ± 3.3 mV and 9.7 ± 0.4 mV for control, and -57.5 ± 6.2 mV and 10.1 ± 0.5 mV for lidocaine. Data were from 3 different cells, first recorded in control buffer and then in lidocaine.

for nicardipine, $n = 5$, $P < 0.01$). Thus, lidocaine has a similar action on inactivation to that of nicardipine. However, with this 5 s conditioning pulse about 40% of control I_{Ba} remained (non-inactivated) which was still sensitive to higher concentrations of lidocaine or nicardipine. Therefore, a 30 s conditioning pulse, which strongly suppressed I_{Ba} above −40 mV, was used to achieve complete steady-state inactivation. Even then, there is a suggestion from the fit of the Boltzmann equation to the data that 5–10% of the current may not inactivate (Fig. 4), consistent with observations made in a different clone of rat anterior pituitary cells (Cohen and McCarthy, 1987). With this longer prepulse, lidocaine (1 mM) inhibited I_{Ba} by 28% at the conditioning potential of −100 mV and shifted the availability function even further to the left, by about 11 mV ($V_{0.5} = -46.8 \pm 3.3$ mV for control, and -57.5 ± 6.2 mV for lidocaine, $n = 3$, $P < 0.01$) compared to only a 7 mV shift when the 5-s prepulse was used. It is also noteworthy that the control availability curve for 30 s long prepulses was left-shifted (by 14 mV) compared to its voltage position for 5 s long prepulses; channels were less available at all potentials and were more susceptible to lidocaine's inhibition when long depolarizations were applied. The non-inactivatable current, persisting after prepulses to 0 mV, was also inhibited by 1 mM lidocaine (Fig. 4). Thus, inactivation is modified by lidocaine, but is not essential for lidocaine's inhibitory action.

The inhibition of the total peak current by 1 mM lidocaine at −100 mV holding potential, 28% of control, corresponds to a $K_d = 2.7$ mM, comparable to the value of 3 mM for resting channels derived above. At the holding potential of −20 mV, where Ca^{2+} channels are ca. 90% inactivated, the inhibition of total I_{Ba} is 64%, corresponding to a $K_d = 0.56$ mM.

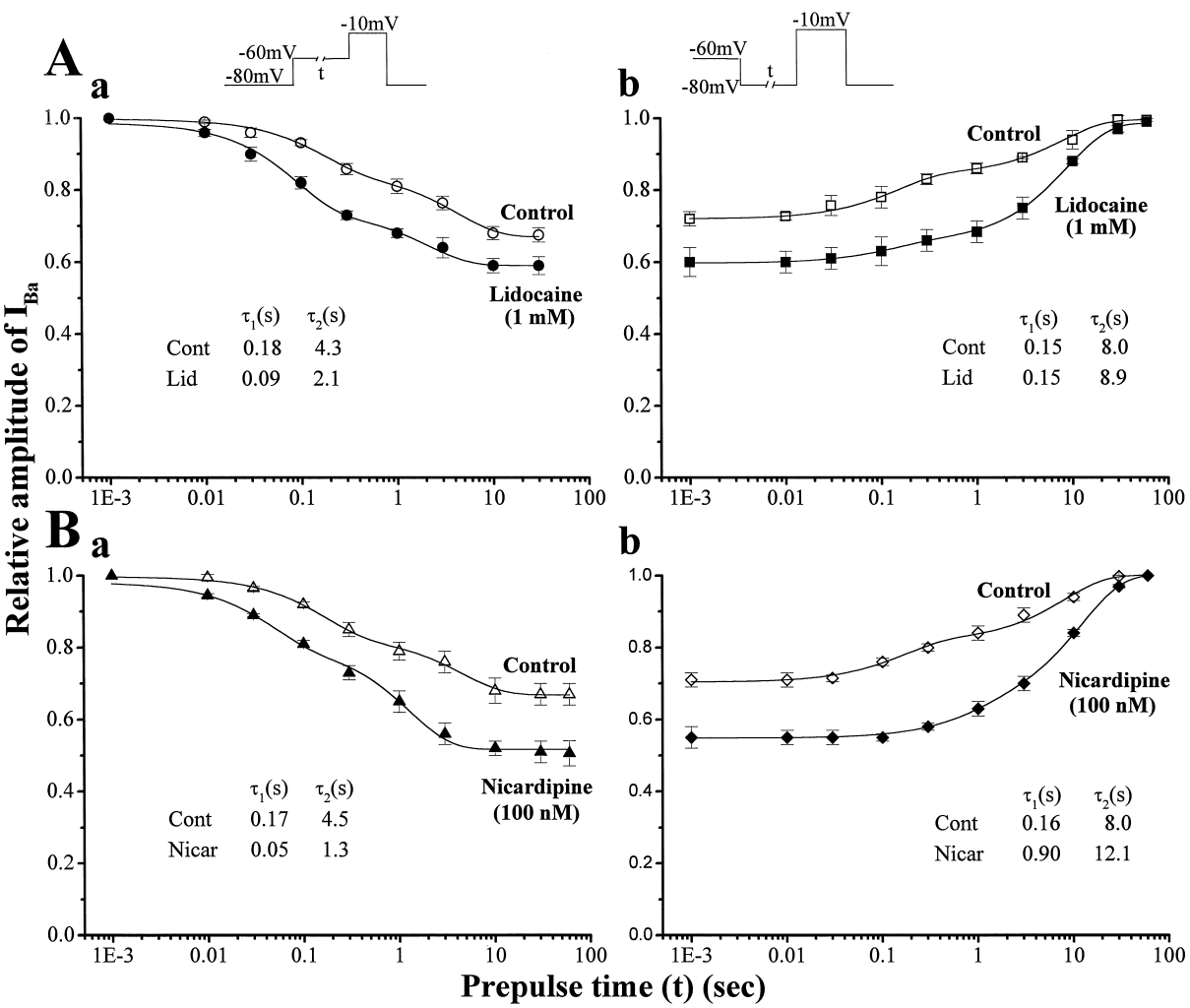

Fig. 5. The kinetics of development and recovery of I_{Ba} inactivation, as altered by lidocaine (A) and nicardipine (B). Experimental voltage patterns are shown at the top of the figure. The maximal I_{Ba} value was used for normalization in each experiment. $_{Aa}$: The loss of availability of peak I_{Ba} during prolonged depolarization to −60 mV is fit by bi-exponential kinetics in the absence (open circles) and presence (filled circles) of 1 mM lidocaine (see text Eq. (5)). (Ab) Recovery of availability I_{Ba} at −80 mV in the absence (open squares) and presence (filled squares) of 1 mM lidocaine also has bi-exponential kinetics. (Ba) Development of and (Bb) recovery from inactivation in 100 nM nicardipine also require 2 exponentials for a good fit. Data were from 5 different cells for each experiment.

3.5. Time constant of Ca^{2+} channel inactivation onset and removal

Since the steady-state voltage-dependent Ca^{2+} channel inhibition by lidocaine differed at 5 and 30 s, the kinetics of the decrease in availability (inactivation) and its recovery were examined. Inactivation kinetics with and without lidocaine were determined using a two-pulse protocol in which the membrane potential was stepped from −80 mV to −60 mV for various durations, and then to a test potential of −10 mV (Fig. 5a). Similarly, the hyperpolarization-induced recovery was determined by imposing a prepulse from −60 mV to −80 mV for various durations, and then a test potential of −10 mV (Fig. 5b). For both procedures, the relative amplitude of I_{Ba} was plotted against the prepulse time, and the time constant was then determined by fitting the curve with exponential functions. The curves for both depolarization-induced I_{Ba} inactivation and hyperpolarization-induced I_{Ba} reactivation were best fit by a sum of two exponentials:

$$I_{Ba} = I_1 \exp(-t/\tau_1) + I_2 \exp(-t/\tau_2) \quad (5)$$

where I_1 and I_2, t and τ_1 and τ_1 are the relative amplitudes of I_{Ba}, time, and time constants, respectively.

As shown in Fig. 5Aa, inactivation developed with two time constants: $\tau_1 = 0.18$ s and $\tau_2 = 4.3$ s. These separable inactivation rates suggest the presence of either two pathways for inactivation or two classes of Ca^{2+} channels. The latter has previously been reported for single channel experiments in GH_3 cells (Mantegazza et al., 1995) and macroscopic current recordings in GH_4C_1 clonal anterior pituitary cells (Cohen and McCarthy, 1987). Lidocaine (1 mM) accelerated both phases of inactivation 2-fold, yielding $\tau_1 = 0.09$ s and $\tau_2 = 2.1$ s. The relative amplitude of the fast inactivation phase (I_1) was selectively increased (control: as fraction of total I_{Ba}, $I_1 = 0.15$, $I_2 = 0.18$; $I_1/I_2 = 0.83$; lidocaine: $I_1 = 0.25$, $I_2 = 0.15$; $I_1/I_2 = 1.67$). However, lidocaine had little effect on the rate constants of recovery from inactivation (Fig. 5Ab) (control: $\tau_1 = 0.15$ s, $\tau_2 = 8.0$ s; lidocaine: $\tau_1 = 0.15$ s, $\tau_2 = 8.9$ s), although the relative amplitudes of the recovery phases were changed (control: $I_1 = 0.12$, $I_2 = 0.15$; $I_1/I_2 = 0.80$; lidocaine: $I_1 = 0.06$, $I_2 = 0.33$; $I_1/I_2 = 0.18$). The rapidly recovering fraction was halved in lidocaine whereas the slowly recovering fraction was doubled.

The effect of nicardipine, a dihydropyridine Ca^{2+} channel antagonist, on I_{Ba} inactivation kinetics was also investigated. As shown in Fig. 5Ba, nicardipine (100 nM) accelerated the depolarization-induced I_{Ba} inactivation by about 3-fold (control: $\tau_1 = 0.17$ s, $\tau_2 = 4.5$ s; nicardipine: $\tau_1 = 0.05$ s, $\tau_2 = 1.3$ s). In addition, the relative amplitude of slowly inactivating I_{Ba} (I_2) was increased (control: $I_1 = 0.17$, $I_2 = 0.16$; nicardipine: $I_1 = 0.18$, $I_2 = 0.29$). However, unlike lidocaine, nicardipine also markedly slowed recovery from inactivation, especially of the rapidly recovering component (Fig. 5Bb) (control: $\tau_1 = 0.16$ s, $\tau_2 = 8.0$ s; nicardipine: $\tau_1 = 0.90$ s, $\tau_2 = 12.1$ s). In addition, the relative amplitudes of recovery phases were changed (control: $I_1 = 0.11$, $I_2 = 0.18$; nicardipine: $I_1 = 0.08$, $I_2 = 0.38$) in a way similar to those changes effected by lidocaine.

3.6. Lack of use-dependence of lidocaine on Ca^{2+} channels

Lidocaine exhibits use-dependent inhibition of the fast Na^+ current in many excitable cells including GH_3 cells (Wang et al., 1995). In the present experiments, the possible use-dependent block by lidocaine of Ca^{2+} channels was examined. Current was evoked by depolarizing the membrane to −10 mV for 30 ms from a holding potential of −80 mV with different frequencies of 1, 2, and 3.3 Hz. Lidocaine (1 mM) inhibited I_{Ba} without use-dependent actions at any of these frequencies (data not shown). This result is consistent with the absence of effect of lidocaine on the kinetics of removal of inactivation (Fig. 6Ab). Thus,

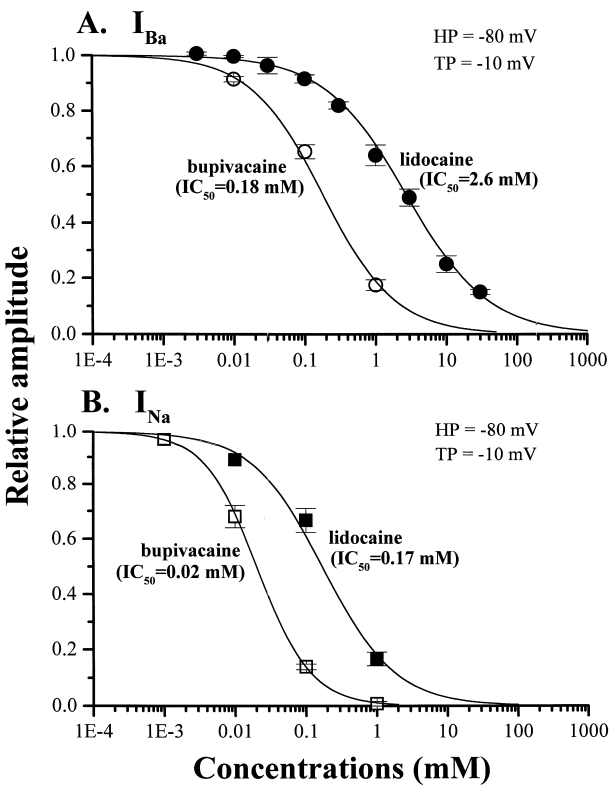

Fig. 6. Comparison of inhibitory potency for lidocaine and bupivacaine on Ca^{2+} and Na^+ channels. (A) Concentration–inhibition curves for bupivacaine (open circles) and lidocaine (filled circles) on Ca^{2+} channels (I_{Ba}) ($n = 5$–12). The data for lidocaine are same as in Fig. 4 (HP of −80 mV). $n_H = 0.9$ and 0.8 for bupivacaine and lidocacine, respectively. (B) Dose-responses of bupivacaine (open squares) and lidocaine (filled squares) on Na^+ channels (I_{Na}). Number of cells were 5 except the points of 0.001 mM for bupivacaine and 0.01 mM for lidocaine, for which the number was 1. Solid lines are nonlinear least squares fits to the data of the Hill equation (see Fig. 4 legend); $n_H = 1.1$ and 0.9 for bupivacaine and lidocaine, respectively.

lidocaine has different inhibitory kinetics on the Ca^{2+} channels and Na^+ channels in GH_3 cells.

3.7. Additive effect of lidocaine and nicardipine on I_{Ba}

Since both lidocaine and nicardipine modify Ca^{2+} channel kinetics, and in quite similar manners, they might bind to the same site on the channel. If that were true, the relative inhibition by lidocaine of I_{Ba} would be expected to be smaller in the presence of nicardipine. However, when 100 nM nicardipine had inhibited I_{Ba} by 50% (holding potential = −80 mV), subsequent application of lidocaine (1 mM) further inhibited the residual I_{Ba} by 37%, an amount virtually identical to that observed in the absence of nicardipine (see Fig. 3). Similarly, simultaneous application of both nicardipine and lidocaine to the bath produced an algebraically additive inhibition (data not shown). Table 1 shows the averaged values of relative inhibition of I_{Ba} by lidocaine, in the absence and presence of two concentrations of nicardipine, and confirms that nicardipine (at 30 or 100 nM) does not modify lidocaine-induced inhibition.

3.8. Comparative potencies for lidocaine and bupivacaine on I_{Ba} and I_{Na}

The inhibitory effects of bupivacaine, another local anesthetic, on Ca^{2+} channels and Na^+ channels were examined and compared with those of lidocaine. Fig. 6A shows the concentration dependence of lidocaine and bupivacaine on I_{Ba} inhibition; the potency of bupivacaine (IC_{50} = 0.18 mM) was 14 times greater than that of lidocaine (IC_{50} = 2.6 mM). In addition, both local anesthetics strongly inhibited the fast Na^+ current in the same cells at 10–20 times their potency on Ca^{2+} channels (Fig. 6B). Again, the potency of bupivacaine (IC_{50} = 0.02 mM) was greater (8 times) than that of lidocaine (IC_{50} = 0.17 mM), although the ratio for the inhibition of I_{Na} was only about half that for I_{Ba} inhibition. Interestingly, there is a smaller ratio of affinities between the two drugs at the target with the higher affinity (I_{Na}) than at the one with lower affinity (I_{Ba}).

Table 1
Relative inhibition[a] by lidocaine of Ca^{2+} channels in GH_3 cells

Lidocaine (1 mM)	% Inhibition of I_{Ba}^b	Number (n)
In 10 mM Ba^{2+} solution	36.0 ± 3.7%	10
In 10 mM Ba^{2+} + 30 nM nicardipine solution	38.6 ± 3.3%	3
In 10 mM Ba^{2+} + 100 nM nicardipine solution	39.0 ± 3.5%	4

[a] % inhibition = $[(I_{CTL} - I_{LID})/I_{CTL}] \times 100$, where CTL refers to an identical but lidocaine-free solution.
[b] All values are mean ± S.E. Holding potential = −80 mV; Testing potential = −10 mV.

4. Discussion

This paper describes the voltage- and time-dependent inhibition of L-type Ca^{2+} channels by local anesthetics, particularly lidocaine. Others have previously noted the inhibition of Ca^{2+} currents by local anesthetics. Lidocaine and procaine inhibited I_{Ca} in snail neurons (Akaike et al., 1982), and lidocaine produced both a tonic inhibition ($IC_{50} \sim 0.3$ mM at holding potential = −60 mV) and a time-dependent inhibition of open channels (Oyama et al., 1988) in isolated frog sensory neurons. These sensory neurons contain mostly N-type Ca^{2+} channels (Bean, 1989) which are inhibited by local anesthetics with about the same potency as for Na^+ channels (Guo et al., 1991; Sugiyama and Muteki, 1994).

In skeletal muscle, local anesthetics effect the Ca^{2+} channels that are located in the transverse tubules (Palade and Almers, 1985). The rank order of potency is: dibucaine ≫ tetracaine > lidocaine > procaine > benzocaine. The IC_{50} for lidocaine was 1.4 mM at a holding potential of −70 mV, close to the value reported here for neuronal cells.

Both Na^+ and Ca^{2+} currents in myocardial tissue are inhibited by local anesthetics. (Josephson, 1988). L-type Ca^{2+} currents of guinea pig are inhibited by tetracaine, but with little effect on the kinetics of inactivation (Carmeliet et al., 1986). The local anesthetic potency in these cardiac cells, held at −40 to −45 mV (IC_{50} = 80 μM), is about twice that for blockade of skeletal muscle Ca^{2+} currents held at −70 mV, IC_{50} = 160 μM (Palade and Almers, 1985). Assuming that only small differences in intrinsic drug potency exist between tissues (but see Walker and De Waard, 1998), these results in skeletal and cardiac muscle show qualitative agreement with the voltage-dependent action of lidocaine in the present study.

There are many similarities between the local anesthetic inhibition of these neuronal Ca^{2+} channels and the well studied inhibition of Na^+ channels, including a 'tonic' block of resting channels and a shift in the voltage-dependence of inactivation with corresponding changes in the rate of recovery from inactivation (Hille, 1977; Hondeghem and Katzung, 1977), consistent with a higher affinity of lidocaine for the inactivated over the resting channel state.

A time- and concentration-dependent inhibition of open Ca^{2+} channels by lidocaine resembled that for open Na^+ channels (Wang et al., 1986). The rate constants for open Ca^{2+} channel blockade were $k_+^O = 2.57 \times 10^3$ M^{-1} s^{-1} and $k_-^O = 2.83$ s^{-1}. The respective lidocaine rate constants for blockade of open Na^+ channels in frog nerve were $k_+ = 1.4 \times 10^5$ M^{-1} s^{-1} and $k_- = 1.3 - 1.5$ s^{-1} (Chernoff, 1990), and in frog muscle $k_+ = 1.7 \times 10^5$ M^{-1} s^{-1}, and $k_- = 1.3 - 1.7$ s^{-1} (Schwarz et al., 1977). It thus appears that lidocaine's affinity for open Ca^{2+} channels is less than that for open Na^+ channels because of a 50-fold slower rate of binding, with only a 2-fold faster rate of

dissociation. The slower blocking rate constant implies a much smaller access pathway or a much reduced local 'free' concentration (e.g., in the membrane, Hille, 1977; Chernoff and Strichartz, 1990). Further evidence for the importance of activation in modulating Ca^{2+} channel block by local anesthetics is found in the voltage-dependence of peak current inhibition (Fig. 1C). In the range of membrane potentials where channel activation increases 4-fold with voltage (20% at −40 mV to 80% at −20 mV), inhibition by lidocaine rises proportionately, from 8% to 32%.

Lidocaine shows a higher affinity for the inactivated forms of both Na^+ and Ca^{2+} channels, but the kinetic basis of this effect differs between channel types. For Na^+ channels the apparent enhancement of the inactivated state results primarily from a slowing of the recovery from inactivation. Recovery of inactivated drug-free Na^+ channels to a state available for gating (the 'resting' state) has both fast and slow components (Khodorov et al., 1976). The presence of local anesthetic lowers the fraction of rapidly recovering channels, producing a new kinetic phase of intermediate recovery rate, with amplitude proportional to local anesthetic concentration (Starmer et al., 1984; Yeh and Tanguy, 1985). There is little effect of local anesthetic on the rate of development of Na^+ inactivation (Strichartz, 1985; Chernoff, 1990). In contrast, lidocaine has more complex effects on Ca^{2+} channel inactivation kinetics. Specifically, the onset of inactivation has two kinetic components in drug-free cells, and each of these is accelerated equally by lidocaine. Noticeably, the inactivation onset spurred by lidocaine is much slower than the open channel inhibition described above (cf. Fig. 2), showing that binding of the drug to the activated channel does not directly result in an inactivated state.

Inactivation recovery also has two phases, but the time constant for neither is changed in lidocaine. Instead the drug shifts the distribution between these phases, halving the fraction of total current with fast recovery while doubling the fraction with slow recovery. The overall effect of lidocaine during a long depolarization appears to be a redistribution of inactivating Ca^{2+} channels between naturally occurring conformations. Nicardipine has similar effects to lidocaine in speeding the onset of inactivation and doubling the fraction that rapidly becomes inactivated. But nicardipine, unlike lidocaine, altered the recovery rates as well of Ca^{2+} inactivation. Fast recovery was slowed almost 6-fold; slow recovery was slowed only by 50%, but the slowly recovering fraction of total current was more than doubled. Nicardipine slows inactivation recovery greatly compared to drug-free channels, whereas lidocaine does not much alter this rate, and it seems likely that this kinetic difference accounts for the overall greater potency of nicardipine.

Viewed from a purely kinetic perspective, the local anesthetic binding can alter the way that inactivating Ca^{2+} channels distribute between slowly and rapidly recovering states, but the drug itself dissociates too rapidly to influence the rate of recovery per se. Dihydropyridine binding similarly alters the channel distribution between inactivated states, but these drugs remain bound to the channel for times long enough to affect recovery rates. It will be interesting to know if other local anesthetics that are more potent than lidocaine on the Ca^{2+} channels are able to change the rates of inactivation or if this property is assumed only by drugs that act at the dihydropyridine site.

Acknowledgements

The authors thank Ms. Laura Krebaum and Ms. Colette Lavoie for cell culture. This work was supported by USPHS GM15904, the Harvard Anesthesia Center Grant, Project IV (to GRS).

References

Akaike, N., Ito, H., Nishi, K., Oyama, Y., 1982. Further analysis of inhibitory effects of propranolol and local anesthetics on the calcium current in Helix neurons. Br. J. Pharmacol. 76, 37–43.

Bean, B., 1989. Neurotransmitter inhibition of neuronal calcium currents by changes in channel voltage dependence. Nature 340, 153–156.

Bezanilla, F., Armstrong, C.M., 1977. Inactivation of sodium channel: II. Gating experiments. J. Gen. Physiol. 70, 567–590.

Bingmann, D., Tetsch, P., Lipinski, H.G., 1987. Effect of lidocaine on action potentials of the soma membrane of sensory spinal ganglion (SSG) cells. Pflug. Arch. 408, R70, Suppl. 1.

Bolger, G.T., Marcus, K.A., Daly, J.W., Skolnick, P., 1987. Local anesthetics differentiate dihydropyridine calcium antagonist binding sites in rat brain and cardiac membranes. J. Pharm. Exp. Ther. 240, 922–930.

Browne, T., Hirota, K., Lambert, D.G., 1996. Is the neuronal dihydropyridine binding site on L-type Ca^{2+} channels a target for local anesthetic agents?. Br. J. Anaesth. 77, 290P.

Butterworth, J.F., Strichartz, G.R., 1990. Molecular mechanisms of local anesthesia: a review. Anesthesiology 72, 711–734.

Carmeliet, E., Morad, M., Van der Heyden, G., Vereecke, J., 1986. Electrophysiological effects of tetracaine in single guinea-pig ventricular myocytes. J. Physiol. 376, 143–161.

Chaplan, S.R., Bach, F.W., Shafer, S.L., Yaksh, T.L., 1995. Prolonged alleviation of tactile allodynia by intravenous lidocaine in neuropathic rats. Anesthesiology 83, 775–785.

Chernoff, D., 1990. Kinetic analysis of phasic inhibition of neuronal sodium currents by lidocaine and bupivacaine. Biophys. J. 58, 53–68.

Chernoff, D.M., Strichartz, G.R., 1990. Kinetics of local anesthetic inhibition of neuronal sodium currents. PH and hydrophobicity dependence. Biophys. J. 58, 69–81.

Cohen, E.N., 1968. Distribution of local anesthetic agents in the neuraxis of the dog. Anesthesiology 29, 1002.

Cohen, C.J., McCarthy, R.T., 1987. Nimodipine block of calcium channels in rat anterior pituitary cells. J. Physiol. 387, 195–225.

Dubinsky, J.M., Oxford, G.S., 1985. Dual modulation of K channels by thyrotropin-releasing hormone in clonal pituitary cells. Proc. Natl. Acad Sci. USA 82, 4282–4286.

Fink, B.R., Cairns, A.M., 1987. Lack of size-related differential sensitivity to equilibrium conduction block among mammalian myelinated axons exposed to lidocaine. Anesth. Analg. 66, 948–953.

Guo, X., Castle, N.A., Chernoff, D.M., Strichartz, G.R., 1991. Comparative inhibition of voltage gated cation channels by local anesthetics.

In: Miller, K., Roth, S., Rubin, E. (Eds.), Annals of N.Y. Academy of Sciences, Vol. 625: Molecular and Cellular Mechanisms of Alcohol and Anesthetic. New York Academy of Sciences, New York, pp. 181–199.

Hamill, O.P., Marty, A., Neher, E., Sackmann, B., Sigworth, F.J., 1981. Improved patch clamp techniques for high resolution current recording from cells and cell-free membrane patches. Pflug. Arch. 391, 85–100.

Hille, B., 1977. Local anesthetics: hydrophilic and hydrophobic pathways for the drug-receptor reaction. J. Gen. Physiol. 69, 497–515.

Hondeghem, L.M., Katzung, B.G., 1977. Time-and voltage-dependent interactions of antiarrhythmic drugs with cardiac sodium channels. Biochim. Biophys. Acta 472, 373–389.

Huang, J.H., Thalhammer, J.G., Raymond, S.A., Strichartz, G.R., 1997. Susceptibility to lidocaine of impulses in different somatosensoty afferent fibers of rat sciatic nerve. J. Pharmacol. Exp. Ther. 292, 802–811.

Johns, R.A., DiFazio, C.A., Longnecker, D.E., 1985. Lidocaine constricts or dilates rat arterioles in a dose-dependent manner. Anesthesiology 62, 141–144.

Josephson, I.R., 1988. Lidocaine blocks Na, Ca, and K currents in chick ventricular myocytes. J. Mol. Cell. Cardiol. 20, 593–604.

Kalman, S., Bjorhn, K.C., Tholen, E.K., Lisander, B., 1997. Mepivacaine as an intravenous reginal block interferes with reactive hyperemia and decreases steady-state blood flow. Reg. Anesth. 22, 552–556.

Kessler, K.M., Kissane, B., Cassidy, J., Pefkaros, K.C., Kozlovskis, P., Hamburg, C., Myerburg, R.J., 1984. Dynamic variability of binding of antiarrhythmic drugs during the evolution of acute myocardial infarction. Circulation 70, 472–478.

Khodorov, B., Shishkova, L., Peganov, E., Revenko, S., 1976. Inhibition of sodium currents in frog Ranvier node treated with local anesthetics. Role of slow sodium inactivation. Biochim. Biophys. Acta 433, 409–435.

Mantegazza, M., Fasolayto, C., Hescheler, J., Pietrobon, D., 1995. Stimulation of single L-type calcium channels in rat pituitary GH_3 cells by thyrotropin-releasing hormone. EMBO J. 14, 1075–1083.

Oyama, Y., Sadoshima, J.-I., Tokutomi, N., Akaike, N., 1988. Some properties of inhibitory action of lidocaine on the Ca^{2+} current of single isolated frog sensory neurons. Brain Res. 442, 223–228.

Palade, P.T., Almers, W., 1985. Slow calcium and potassium currents in frog skeletal muscle: their relationship and pharmacologic properties. Pflug. Arch. 405, 91–101.

Partridge, B.L., 1991. The effect of local anesthetics and epinephrine on rat sciatic nerve blood flow. Anesthesiology 75, 243–251.

Rossner, K.L., Freese, K.J., 1997. Bupivacaine inhibition of L-type calcium current in ventricular cardiomyocytes of hamster. Anesthesiology 87, 926–934.

Schwarz, W., Palade, P.T., Hille, B., 1977. Local anesthetics: effect of pH on use-dependent block of sodium channels in frog muscle. Biophys. J. 20, 343–368.

Starmer, C.F., Grant, A.O., Strauss, H., 1984. Mechanisms of use-dependent block of sodium channels in excitable membranes by local anesthetics. Biophys. J. 46, 15–28.

Strichartz, G.R., 1985. Interactions of local anesthetics with neuronal sodium channels. In: Covino, B., Fozzard, H.A., Rehder, K., Strichartz, G.R. (Eds.), Effects of Anesthesia, Clinical Physiology. American Physiological Society, Bethesda, pp. 39–52.

Sugiyama, K., Muteki, T., 1994. Local anesthetics depress the calcium current of rat sensory neurons in culture. Anesthesiology 80, 1369–1378.

Taylor, R.E., 1959. Effect of procaine on electrical properties of squid axon membrane. Am. J. Physiol. 196, 1071–1078.

Walker, D., De Waard, M., 1998. Subunit interaction sites in voltage-dependent Ca^{+2+} channels: role in channel function. Trends Neurosci. 21, 148–154.

Wang, G.K., Brodwick, M.S., Eaton, D.C., Strichartz, G.R., 1986. Inhibition of sodium currents by local anesthetics in chloramine-T-treated squid axons. The role of channel activation. J. Gen. Physiol. 89, 645–667.

Wang, G.K., Quan, C., Vladimirov, M., Mok, W.M., Thalhammer, J.G., 1995. Quaternary ammonium derivative of lidocaine as a long-acting local anesthetic. Anesthesiology 83, 1293–1305.

Weidmann, S., 1955. Effect of calcium ions and local anesthetics on electrical properties of Purkinje fibers. J. Physiol. (London) 129, 568–582.

Wulf, H., Godicke, J., Herzig, S., 1994. Functional interaction between local anesthetics and calcium antagonists in guinea pig myocardium: 2. Electyrophysiological studies with bupivacaine and nifedipine. Br. J. Anesth. 73, 364.

Xiong, Z.L., Strichartz, G.R., 1995. Inhibition by local anesthetics of calcium channels in anterior pituitary cells. Biophys. J. 68, A209.

Yeh, J.Z., Tanguy, J., 1985. Na channel activation gate modulates slow recovery from use-dependent block by local anesthetics in squid giant axones. Biophys. J. 47, 685–694.